The Astrophysical Journal, 825:20 (10pp), 2016 July 1 doi:10.3847/0004-637X/825/1/20

LOW SURFACE BRIGHTNESS IMAGING OF THE MAGELLANIC SYSTEM: IMPRINTS OF TIDAL INTERACTIONS BETWEEN THE CLOUDS IN THE STELLAR PERIPHERY

Gurtina Besla[1], David Martínez-Delgado[2], Roeland P. van der Marel[3], Yuri Beletsky[4], Mark Seibert[5], Edward F. Schlafly[6,8], Eva K. Grebel[2], and Fabian Neyer[7]
[1] Steward Observatory, University of Arizona, 933 North Cherry Avenue, Tucson, AZ 85721, USA; gbesla@email.arizona.edu
[2] Astronomisches Rechen-Institut, Zentrum für Astronomie der Universität Heidelberg, Mönchhofstr. 12-14, D-69120 Heidelberg, Germany
[3] Space Telescope Science Institute, 3700 San Martin Drive, Baltimore, MD 21218, USA
[4] Las Campanas Observatory, Carnegie Institution of Washington, Colina el Pino, 601 Casilla, La Serena, Chile
[5] Carnegie Observatories, 813 Santa Barbara St, Pasadena, CA 91101, USA
[6] Lawrence Berkeley National Laboratory, One Cyclotron Road, Berkeley, CA 94720, USA
[7] ETH Zurich, Institute of Geodesy and Photogrammetry, 8093 Zurich, Switzerland
Received 2016 February 8; revised 2016 April 11; accepted 2016 May 2; published 2016 June 27

ABSTRACT

We present deep optical images of the Large and Small Magellanic Clouds (LMC and SMC) using a low cost telephoto lens with a wide field of view to explore stellar substructure in the outskirts of the stellar disk of the LMC ($<10^\circ$ from the LMC center). These data have higher resolution than existing star count maps, and highlight the existence of stellar arcs and multiple spiral arms in the northern periphery, with no comparable counterparts in the south. We compare these data to detailed simulations of the LMC disk outskirts, following interactions with its low mass companion, the SMC. We consider interaction in isolation and with the inclusion of the Milky Way tidal field. The simulations are used to assess the origin of the northern structures, including also the low density stellar arc recently identified in the Dark Energy Survey data by Mackey et al. at $\sim 15^\circ$. We conclude that repeated close interactions with the SMC are primarily responsible for the asymmetric stellar structures seen in the periphery of the LMC. The orientation and density of these arcs can be used to constrain the LMC's interaction history with and impact parameter of the SMC. More generally, we find that such asymmetric structures should be ubiquitous about pairs of dwarfs and can persist for 1–2 Gyr even after the secondary merges entirely with the primary. As such, the lack of a companion around a Magellanic Irregular does not disprove the hypothesis that their asymmetric structures are driven by dwarf–dwarf interactions.

Key words: galaxies: dwarf – galaxies: interactions – Galaxy: kinematics and dynamics – Magellanic Clouds

Supporting material: animation

1. INTRODUCTION

The Large and Small Magellanic Clouds (LMC and SMC, respectively) are our closest example of an interacting pair of dwarf galaxies. Evidence of this interaction is clearly illustrated by the existence of the gaseous Magellanic Bridge connecting the Clouds (Kerr 1957; Hindman et al. 1963), and the tail of gas that trails them known as the Magellanic Stream (Mathewson et al. 1974; Putman et al. 2003; Nidever et al. 2010). However, signatures of this interaction history are less clear in their stellar components.

On-going star formation in the LMC is stochastic, giving the dwarf galaxy an irregular appearance in the optical. For example, young, classical cepheids and binary stars trace out a single dominant spiral arm (Moretti et al. 2014). In contrast, near-IR surveys suggest that its older stellar population is smoothly distributed. The Two Micron All Sky Survey (2MASS) and Deep Near-infrared southern Sky Survey data for the LMC reveal a barred galaxy with a smooth old disk, extending to at least 9 kpc in radius (van der Marel 2001). This is similarly revealed by the smooth distribution of RR Lyrae stars in the LMC disk (Haschke et al. 2012).

Asymmetries in the stellar disk do exist, however: the disk appears to be warped (van der Marel & Cioni 2001; Olsen & Salyk 2002; Nikolaev et al. 2004) and the stellar bar of the LMC is geometrically off-center and warped relative to the disk plane (Subramaniam 2003; Lah et al. 2005; Koerwer 2009). 3D maps of the LMC created using Cepheids and RR Lyrae illustrate that the bar is in fact protruding from the disk (Nikolaev et al. 2004; Haschke et al. 2012). This can be explained if the SMC recently collided (impact parameter <5 kpc) with the LMC disk (Besla et al. 2012). This picture is supported by the discovery of low metallicity stars with distinct kinematics, consistent with SMC debris, in the LMC field (Kunkel et al. 1997; Graff et al. 2000; Olsen et al. 2011; Casetti-Dinescu et al. 2012).

Models reproducing these asymmetric features in the LMC and the large scale gaseous structure of the Magellanic System require repeated tidal encounters between the LMC–SMC (e.g., Besla et al. 2010; Diaz & Bekki 2011). Furthermore, the existence of the Magellanic Bridge implies that they must have had at least one close encounter in the recent past—indeed the proper motion vectors force such an encounter (Růžička et al. 2010; Kallivayalil et al. 2013). Evidence of these tidal perturbations from the SMC should be more pronounced in the outer periphery of the stellar disk of the LMC, where the gravitational potential is shallower.

Deep optical surveys of the stellar periphery of the Clouds are underway with OGLE-IV (Udalski et al. 2015) and the Dark Energy Camera on the Blanco 4 m Telescope, notably by the Dark Energy Survey (DES) and the Survey of the Magellanic Stellar History (SMASH). Such studies have revealed the presence of new dwarf galaxies, some of which may be companions (Bechtol et al. 2015; Drlica-Wagner et al.

[8] Hubble Fellow.

2015; Koposov et al. 2015; Martin et al. 2015), and stellar substructure that may trace the hierarchical assembly of the Clouds (Belokurov & Koposov 2016). Such studies are complemented by ongoing surveys of the inner regions of the Clouds, such as the VISTA survey of the Magellanic Clouds (Rubele et al. 2015).

Intriguingly, the DES survey (Balbinot et al. 2015) and previous studies such as the Outer Limit Survey (Saha et al. 2010) have also demonstrated that the LMC's stellar disk extends much farther than the 9 kpc radius revealed by earlier near-IR studies, potentially stretching as far as the Carina dwarf spheroidal galaxy, some 15°–20° away (Muñoz et al. 2006; McMonigal et al. 2014; Mackey et al. 2015). This implies that the disk of the LMC extends at least 30 kpc in diameter. The tenuous periphery of such an extended structure is the ideal location to search for signatures of tidal perturbations from either the Milky Way or its binary companion, the SMC. Such evidence can be used to constrain the tidal radius, and thereby the mass of the LMC, and is critical to constraining the interaction history with both the Milky Way and the SMC.

Recently, a potential stellar stream or arc was identified in the DES data in the northern outskirts of the LMC disk, ∼15° from the LMC center (Mackey et al. 2015), stretching to the east. The authors suggest that this structure may be a result of Milky Way tides acting on the stellar outskirts of the LMC disk (see also, van der Marel 2001). As their simulations illustrate (Mackey et al. 2015, Figure 12 in), in such a scenario, both the northern and southern sections of the disk are affected: there should be a matching structure in the south that stretches to the west. The DES footprint does not extend to that section of the sky and the SMASH survey consists of a discrete set of non-contiguous pointings, which will be unlikely to pick out such faint structures. In the near future, the DECam Magellanic Satellites Survey (PI: Bechtol) will extend the DES footprint to cover the southern LMC disk; this study may be able to shed more light on this question.

The DES results have not provided new information about the structure of the LMC's disk in the inner regions where the stellar density is higher. The seminal optical observations of the LMC by de Vaucouleurs & Freeman (1972) (hereafter deVF72) revealed that the LMC possesses pronounced multi-armed spiral structure in its northern stellar periphery. While the data quality is poor, these maps reveal that the outskirts of the LMC disk are not as smooth as the IR maps suggest. These spiral structures continue to the outskirts of the disk and may play an important role in the origin of the structures observed by Mackey et al. (2015). Such details may be smoothed out in the DES maps. To address the nature of the northern arcs in the LMC disk, we thus require a different observing strategy than that employed to date.

Ultra-deep, wide-field imaging using amateur telescopes can provide an alternative solution to map out substructure in the LMC disk out to large radii. These small-size telescope data trace the substructures as diffuse light features, similar to the approach used in the stellar stream survey undertaken with similar facilities (Martínez-Delgado et al. 2010), with a typical surface brightness limit of 28.5 and 28 mag arcsec^{-2} in g and r. This is approximately three magnitudes deeper than the Sloan Digital Sky Survey II images. In particular, our team has mapped the stellar periphery of analogous systems at much larger distances, such as the starbursting Magellanic Irregular galaxy, NGC 4449. Using a small robotic telescope (0.5 m of aperture) and an exposure time of 18 hr in a luminance filter of the NGC 4449 system, Martínez-Delgado et al. (2012) revealed the existence of a faint stellar stream that may be the remains of a disrupted low mass companion (half the mass of the SMC) orbiting about an LMC-mass dwarf galaxy located ∼4 Mpc away (see their Figure 1). Given the proximity of the Magellanic Clouds to the Milky Way (∼50 kpc away), this observing strategy should also successfully reveal substructure in the stellar periphery of the Clouds, with the advantage of simultaneously imaging the entire Magellanic System—including the entirety of both the LMC and SMC.

Although these data are not as deep as the stellar density maps constructed from stellar tracers (blue horizontal branch or turnoff main sequence stars) selected in SMASH or DES color–magnitude diagrams, they serve an independent and complementary role of revealing substructure in the inner regions of the LMC's disk and how such structure may propagate to the very outskirts.

In what follows we present the first results of our panoramic imaging of the Magellanic System (Section 2) and compare these observations with simulations of the LMC disk that include repeated interactions with the SMC, with and without the tidal effects of the Milky Way (Section 3) Our goal is to address the degree to which the northern arcs are seen in the south and whether interactions between the Clouds can reproduce the extent and degree of asymmetry observed without relying on the tidal influence of the Milky Way. Ultimately, we illustrate that such structures are to be expected around dwarf galaxy pairs in general (Section 4).

2. A DEEP OPTICAL VIEW OF THE MAGELLANIC SYSTEM

Our deep optical program makes use of small robotic telescopes, which provide long exposures at low cost. This observational strategy has been used successfully to detect faint stellar streams about Milky Way analogs, as outlined in Martínez-Delgado et al. (2008, 2010), Amorisco et al. (2015) and about dwarf hosts (Martínez-Delgado et al. 2012).

The deep optical imaging of the LMC and SMC fields presented here were obtained during a pilot optical program devoted to the search of stellar substructure around some Milky Way dwarf satellites. Our observational strategy was designed to provide unresolved images of these stellar systems, tracing their possible streams and other stellar substructures in their periphery by means of diffuse light detection. In addition, to avoid the foreground star and background galaxy contamination problems affecting the stellar density maps, we have adopted a technique that provides a fast (e.g., a single pointing) and cheap way to explore the periphery of these nearby galaxies, similar to those used in ultra-deep imaging of galaxies situated at some tens of Mpc away (e.g., Mihos et al. 2005; Martínez-Delgado et al. 2010; Abraham & van Dokkum 2014; van Dokkum et al. 2014, 2015; Duc et al. 2015). Given that the distance of our targets is always less than some hundreds of kpc, we need to use very short-focal ratio instruments (i.e., $f/3$ or less) to avoid resolving the system into individual stars. In some cases, this low resolution requirement means to use a high quality telephoto lens or apochromatic refractor telescopes, which, in the majority of the cases, is installed on a portable mount working in a very dark site. More details about this project and observational strategy will be available in an

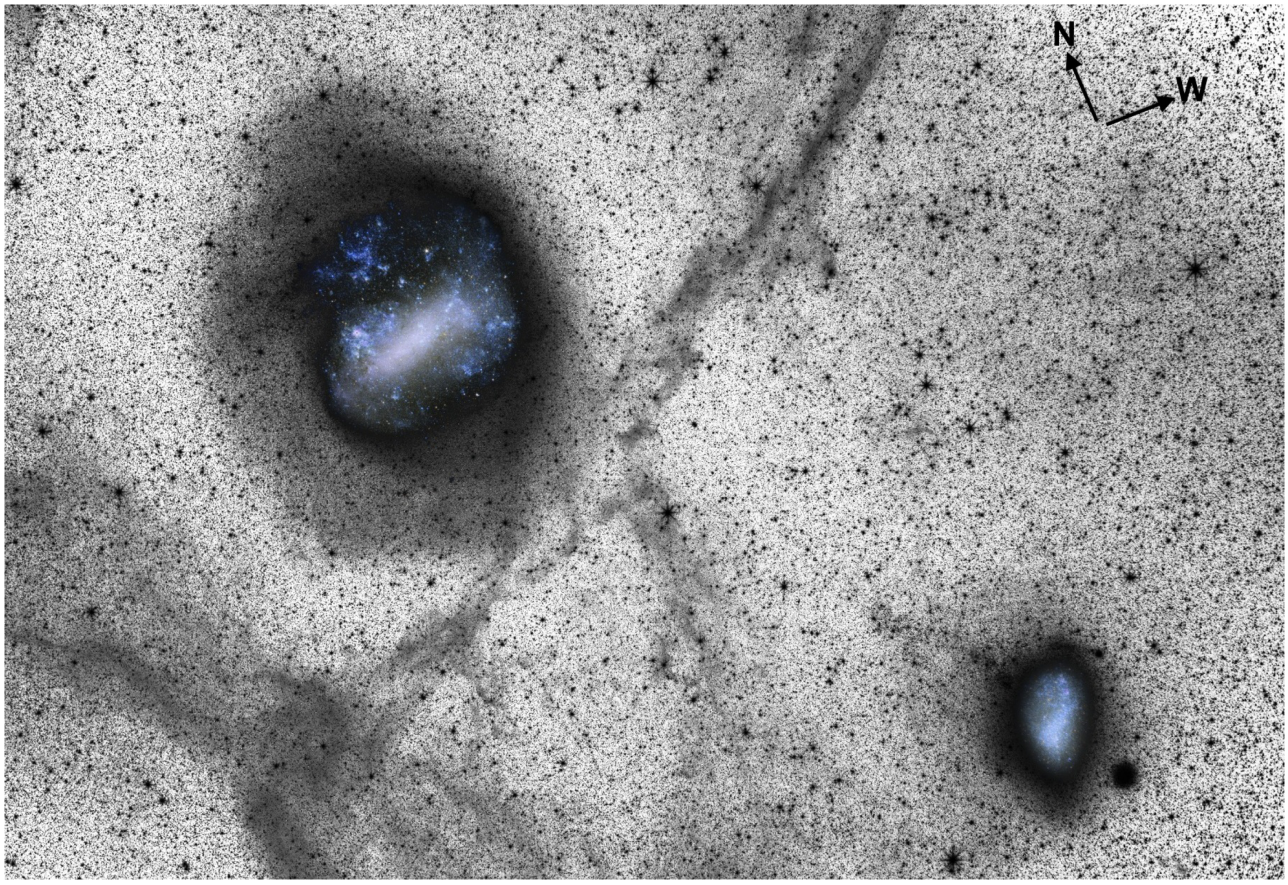

Figure 1. Wide-field Luminance filter image of the Magellanic System (39° × 27°). The LMC is located toward the top left and the SMC is to the bottom right. The Milky Way globular cluster 47 Tuc is visible to the west of the SMC. A tail of stars from the SMC is visible stretching toward the LMC in the east. The outskirts of the LMC disk display pronounced asymmetries. For illustrative purposes, a color inset of the inner regions of the LMC and SMC, made from the color data obtained in our observing run (see Section 2), is inserted as a reference and for comparison with previous studies.

upcoming paper (D. Martínez-Delgado et al. 2016, in preparation).

The imaging data of the LMC and SMC fields described in the following sections was obtained during two observing runs in 2009 August and September at ESO La Silla observatory. The imaging was done using a portable setup consisting of a SBIG STL-11000M CCD camera and Canon prime lenses: Canon EF 50 mm $f/1.4$ USM and Canon EF 200 mm $f/2.8$ L II USM, which yield the FOVs of 39° × 27° and 10° × 7° respectively. The corresponding pixel scales are $37''$ pixel^{-1} and $9\farcs27$ pixel^{-1} accordingly. Each image set consists of deep multiple exposures obtained with a Baader Luminance filter (4000 Å $< \lambda <$ 7500 Å). For each pointing we also obtained a set of images with Baader red, green, and blue filters. The individual exposure time in the Luminance filter was 300 s (for Canon EF 200 mm $f/2.8$ L II USM lens) and 600 s (for Canon EF 50 mm $f/1.4$ USM lens). Standard data reduction procedures for bias subtraction and flat-fielding were carried out using the CCDRED package in IRAF.

2.1. Panoramic View of the Magellanic System

Figure 1 shows a zoomed section of the panoramic view of the Magellanic System made using the Canon EF 50 mm $f/1.4$ USM lens (D. Martínez-Delgado et al. 2016, in preparation). To the west of the SMC is the globular cluster 47 Tuc. To the east of the SMC a tail of young stars extending ∼6° toward the LMC is discernible. These stars are situated in the Magellanic Bridge and are most likely forming in situ, rather than being tidally stripped (Harris 2007).

The LMC shows asymmetric structure in its outskirts that is more pronounced in the north (opposite to the direction of the SMC). These structures will be discussed in more detail in Section 2.2.

Many of the structures visible in the image are Galactic cirrus, which are abundant at high galactic latitude in deep imaging with surface brightness limits fainter than 28 mag arcsec^{-2}. Some of these cirrus features (like the collimated filament between the LMC and the SMC) were previously detected in the photographic plate by de Vaucouleurs & Freeman (1972). We use the dust map of Schlegel et al. (1998) to disentangle surface-brightness features caused by dust from features in the stellar density. These are highlighted in red in the left panel of Figure 2. The map is based on far-infrared observations from IRAS and DIRBE, which are used to estimate the dust column density from its brightness and temperature. The map fails to accurately track the dust column within the Large Magellanic Cloud, where the temperature structure along each line of sight is more complicated than the single, constant temperature assumed by Schlegel et al. (1998). However, the map still qualitatively traces the dust throughout the region, allowing identification of regions and features unaffected by the dust. From these maps it is clear that cirrus does not strongly affect the identification of structure in the LMC outskirts.

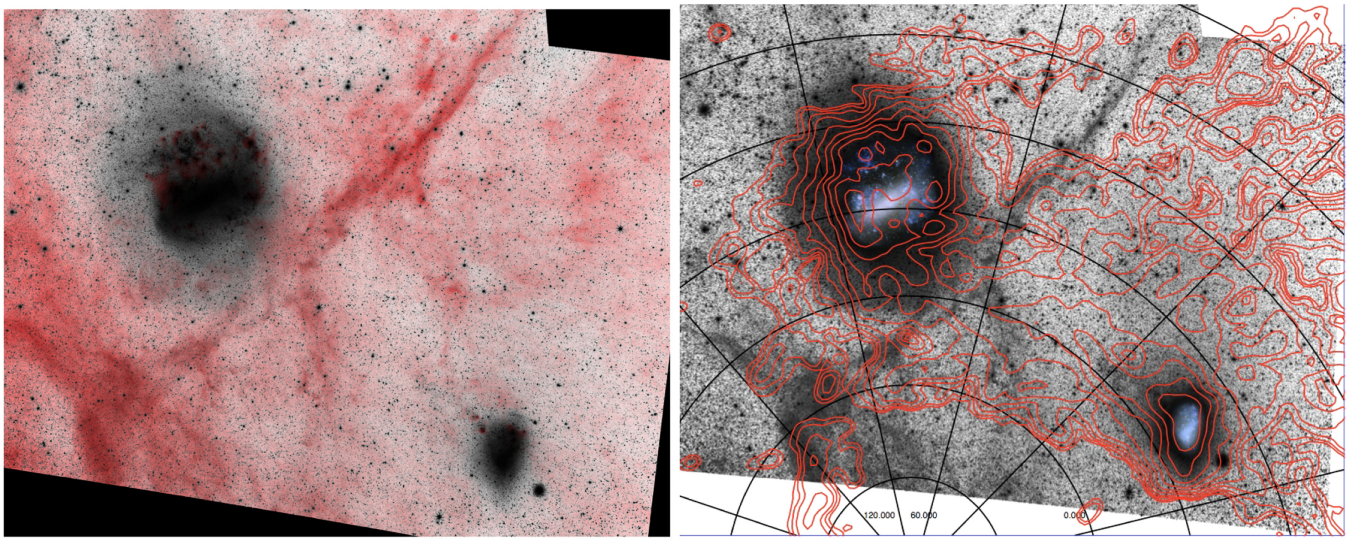

Figure 2. Left: same as Figure 1 where Galactic cirrus, identified based on far-IR observations by IRAS and DIRBE, is highlighted in red. There is very little cirrus in the outskirts of the LMC disk. Right: same with HI contours from (Putman et al. 2003) overplotted. Column densities range from 10^{19} to 10^{21} atoms cm^{-2}. There is a sharp drop in gas density in the LMC outskirts toward the north east (top left), which was modeled in Salem et al. (2015) as an effect induced by ram pressure.

The extended structures discussed in this paper are also seen in maps of stellar clusters, as illustrated by Bica et al. (2008) and Kontizas et al. (1990), confirming that they are not artifacts of the image processing or Galactic cirrus.

In the right panel of Figure 2, HI contours using data from Putman et al. (2003) are plotted over the optical panorama in Figure 1. The tail of young stars from the SMC is located in the highest column density regions of the bridge.

There is a sharp drop off in the gas density toward the upper left (north east), which is the LMC's direction of motion. Our data illustrates that the stellar disk extends beyond this gas truncation radius. This is likely the result of ram pressure stripping as the LMC moves through the circumgalactic medium (Salem et al. 2015). Signatures of this process are likely visible in the truncation time of star formation in the outskirts of the LMC (Meschin et al. 2014), particularly at the larger distances probed by DES.

There is a similar drop off in gas density to the south east of the SMC (Pearson et al. 2016). While our data does not suggest the main body of the SMC extends beyond this radius, Nidever et al. (2011) have illustrated that SMC stars extend to radii as large as 11 kpc, well beyond this gas drop off radius of a few kpc.

2.2. The Large Magellanic Cloud

In this section we focus on the LMC in more detail. With that purpose, we use a higher resolution (9.3 arcsec pixel^{-1}) image obtained with the Canon EF 200 mm $f/2.8$ lens. Plotted in the right hand panel of Figure 3 is the resulting $\sim 20^\circ \times 20^\circ$ Luminance filter image of the LMC. The agreement between the observed morphological perturbations in the northern periphery of the LMC in this independent image and those in Figure 1 confirms that they are not related to artifacts or background fluctuations (e.g., reflections or flat fielding artifacts) from the data.

Figure 3 shows a comparison of the diffuse light structures visible in our deep image (right panel) with the 2MASS star count data (left hand panel van der Marel 2001). In the center panel, contours from the 2MASS data are plotted over our Canon 50 image data. The 2MASS map involves a significant amount of smoothing, since the stellar density of red stars in the LMC outskirts is low. Moreover, only old and intermediate-age (RGB and AGB) stars in the LMC were stacked to create the 2MASS maps.

Our data reaches a similar depth and extent as the 2MASS map. Based on the surface brightness profile presented in Saha et al. (2010), this depth corresponds to $\sim$27 mag arcsec^2. The new direct image (right panel, Figure 3) reveals much more detail in the stellar disk than the 2MASS data. Multiple "embryonic" arms are seen north of the dominant spiral arm, as noted by deVF72. A pronounced stellar arc is visible $\sim 8^\circ$ north of the center of the LMC. These structures are barely visible in the deVF72 maps and are referred to as "semi-detached outlying fragments of spiral arcs" (their region D). The star β-Doradus is seen in projection in the center of the northernmost arc. deVF72 suggest that this arc may be limited on the west and east sides by Galactic cirrus, but Figure 2 indicates this is unlikely.

Pronounced spiral structure is markedly lacking in the south. However, a weak "sub-dominant" arm is seen just south of the bar (referred to as the B1 and B3 regions in deVF72). This appears to be the only southern counterpart to the northern spiral structures. The relative strength of the northern versus southern spiral structures is an important observational constraint for modeling efforts aimed at understanding the origin of these structures (see Section 3).

In Figure 4 we illustrate a modified version of Figure 2 in Mackey et al. (2015) with our color image of the LMC. Our data (marked as region C) do not extend as far as the DES star count data (which stretches to radii of 15°), but they illustrate that structures reminiscent of streams or arcs in the north begin at much smaller radii and do not have counterparts in the south. In particular, there are no prominent streams that extend toward the west (right) in the south, suggesting that the northern structures are unlikely to arise owing to a global tidal field from the Milky Way.

We have marked three important regions in the DES data maps: (A) The northern-most arc or stream (B) intermediate area between our data and the arc, where the stellar disk drops

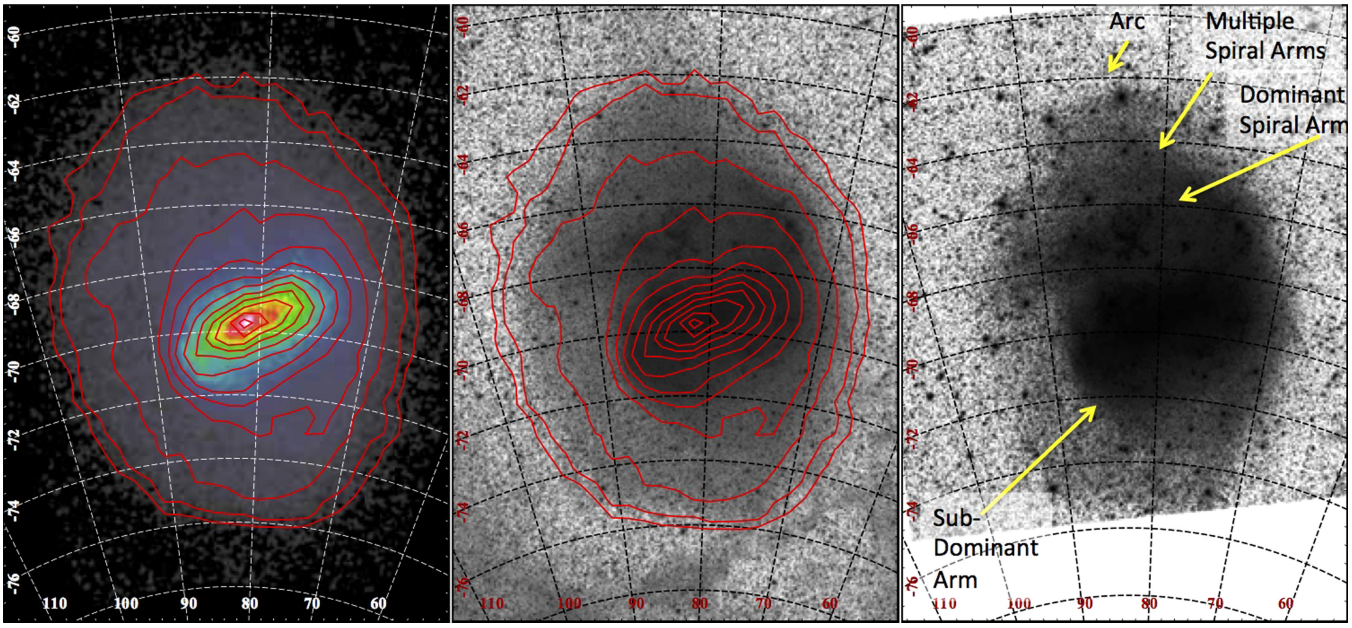

Figure 3. Left: 2MASS near-IR star count map from van der Marel (2001). Contours extend to 8° from the LMC center. Center: our LMC Luminance filter data with 2MASS contours over plotted. Right: luminance filter image, detailing the structure of the LMC. Multiple "embryonic" arms appear to the north of the dominant spiral arm. The northernmost structure appears to be a pronounced stellar arc. Comparable structures do not exist in the south, except for the existence of a "sub-dominant" arm emanating from the bar; this structure is neither as pronounced nor extends as far as the northern spiral structures. The stream found in the DES data by Mackey et al. (2015) is located above the top edge of these figures (see Figure 4).

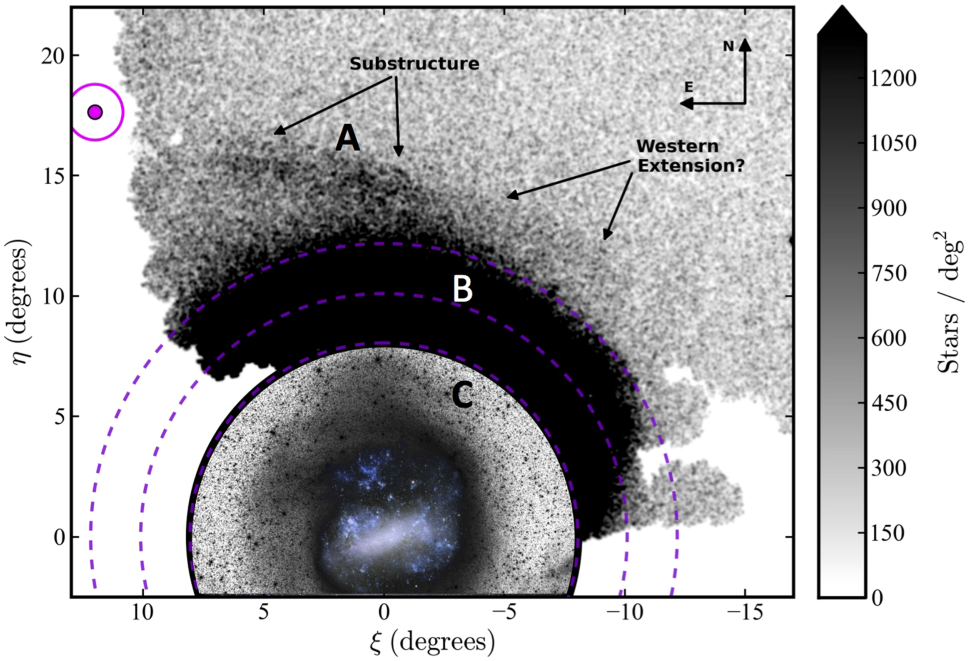

Figure 4. A modified version of Figure 2 from Mackey et al. (2015) showing the spatial density of old main sequence turn-off stars in the LMC. The three purple dashed circles indicate angular separations of 8°, 10° and 12° from the center of the LMC. The stellar stream identified by Mackey et al. (2015) is marked as region A and extends toward the Carina dwarf (magenta point). Our data extends to ∼8°. The substructure we have identified in the LMC is marked as region C. The intermediate region between our data and the DES arc is marked as region B.

off sharply, (C) regions that overlap with our data. We now turn to simulations to interpret the origin of substructure in these regions.

3. COMPARISON WITH SIMULATIONS

Besla et al. (2012, hereafter B12) postulate that asymmetric spiral structure in the LMC results from tidal interactions with the SMC, rather than interactions with the Milky Way. They further argue that this scenario is generically applicable to Magellanic Irregulars in the field. Thus, LMC analogs, regardless of environment, should also have (or once had) low mass companions.

In the following, we explore the structural evolution of the LMC by examining simulations of the interaction and eventual merger of an isolated LMC and SMC binary pair of dwarfs

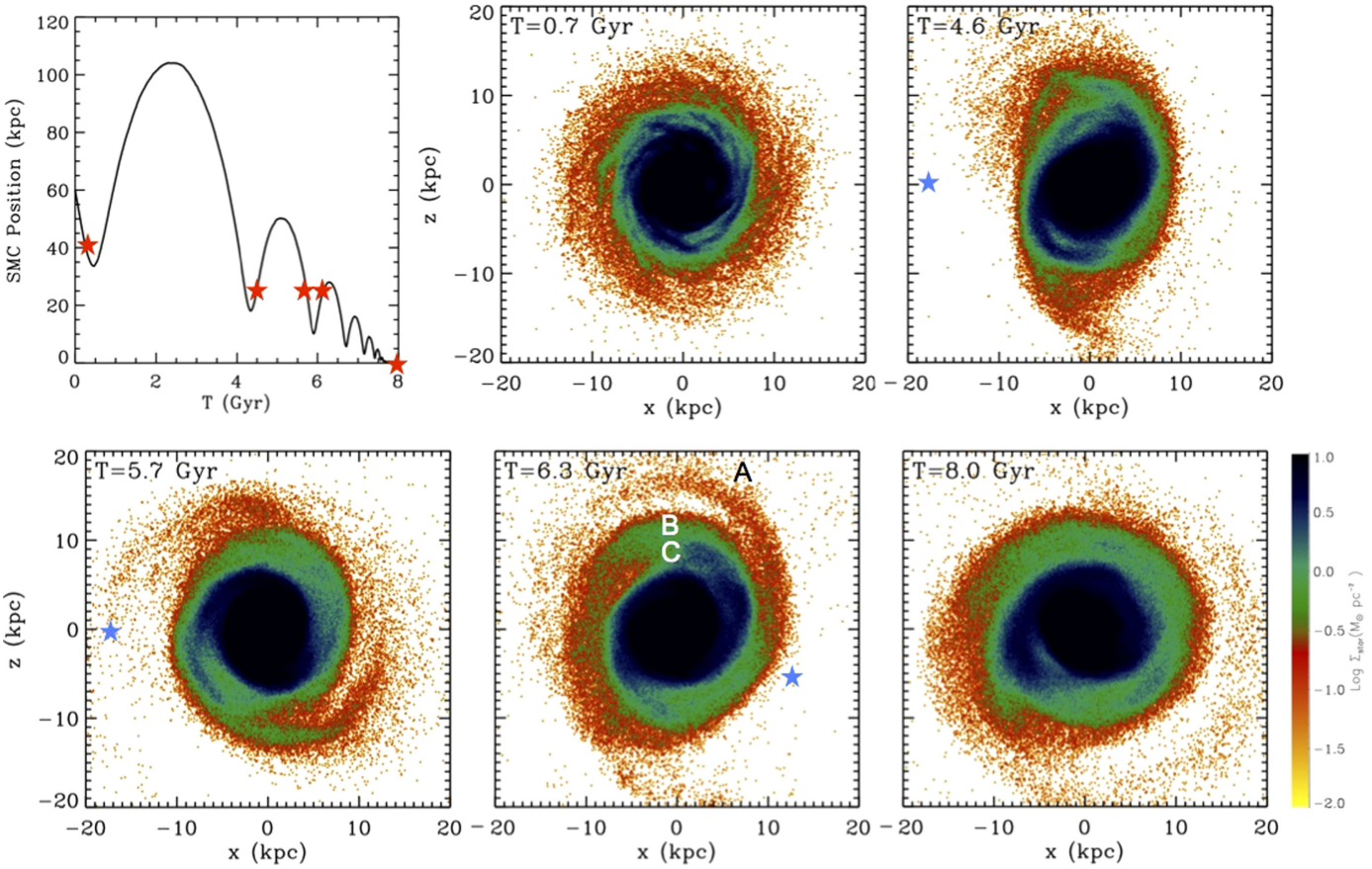

Figure 5. The simulated interaction history of the Large and Small Magellanic Clouds in isolation (i.e., without the Milky Way). The top left panel illustrates the separation between the SMC and LMC as a function of time. The Clouds were likely captured by the Milky Way after 5 or 6 Gyr of evolution as an isolated binary pair. However, here the simulation is followed past that point until the system merges, as would have happened had the Clouds never been captured. Stellar density maps of the LMC disk are plotted at key moments in the interaction history as denoted by red stars in the top left panel. $T = 0.7$ Gyr represents the initial state of the LMC disk as a symmetric exponential disk. At $T = 4.6$, 5.7, and 6.3 Gyr the SMC is roughly 25 kpc from the LMC, as it is today. SMC particles have been omitted from these maps, but the rough location of the SMC is marked by a blue star if it is visible in the field of view. After 6.3 Gyr of evolution the SMC has just passed through the disk of the LMC ($b < 10$ kpc), inducing strong asymmetrical spiral structure and arcs (Region C) that exist as far as 15 kpc from the LMC center (Region A). This structure is similar to that seen in Mackey et al. (2015), illustrating that low density arcs can form at large radii from the LMC center without the influence of the Milky Way tidal field. After 8 Gyr of evolution the system has completely merged, yet asymmetric spiral structure still persist.

(An animation of this figure is available.)

(1:10 mass ratio encounter; Section 3.1). We then explore how the resulting structures might be affected by the large scale tidal field of the Milky Way as the Clouds approach our Galaxy for the first time, by revisiting the simulations presented in B12 (Section 3.2). Specifically, we focus on the structure of the stellar periphery of the LMC as it interacts with the SMC and compare these structures with the high resolution data presented in this paper.

3.1. The LMC and SMC in Isolation

We begin by examining the impact of tidal perturbations on the LMC stellar periphery owing to repeated, prograde, roughly polar orbits of the SMC about an otherwise isolated LMC. We created simulations of this interaction using the smoothed particle hydrodynamics code, GADGET-3 (Springel 2005). These simulations were then used in B12 to model the evolution of the Clouds before they were captured by the Milky Way.

Simulation parameters are outlined in detail in Section 2 of B12. The Clouds are both modeled with exponential stellar and gas disks and live Hernquist dark matter halos. The stellar mass of the simulated LMC is initially 2.5×10^9 $M_\odot$, its gas mass is 1.1×10^9 $M_\odot$ and its total dark matter mass is 1.8×10^{11} $M_\odot$, consistent with expectations from ΛCDM (Besla et al. 2010; Boylan-Kolchn et al. 2011; Moster et al. 2013; Besla 2015; Gómez et al. 2015; Peñarrubia et al. 2016).

The stellar mass of the simulated SMC is initiallly 2.6×10^8 $M_\odot$, its gas mass is 7.9×10^8 $M_\odot$ and total dark matter mass is 2.1×10^{10} $M_\odot$. See Table 1 of B12 for full details of the numerical set up. This simulation accounts for star formation and thus the stellar mass increases over time, roughly approximating the current stellar mass of the Clouds today after ~6–7 Gyr of evolution.

The SMC is placed on a roughly polar, eccentric orbit about the LMC (eccentricity of 0.7), which slowly decays over time owing to dynamical friction. The separation between the galaxies is plotted as a function of time in the top left panel of Figure 5. This figure is an extension of the orbit shown in Figure 2 of B12. In B12, the binary pair followed a trajectory that entered the Milky Way's virial radius after roughly 5 or

6 Gyr. Here instead, we keep the LMC and SMC pair in isolation and allow the binary to evolve further in time until the SMC is eventually completely cannibalized by the LMC (after 8 Gyr of evolution). This represents the ultimate fate of the Magellanic Clouds if they had never been captured by the Milky Way and may mimic the evolution of pairs of dwarfs in the field. The structures produced are therefore independent of the Milky Way's tidal field.

The color panels in Figure 5 illustrate the structure of the LMC stellar disk, seen face on, at various times in the SMC's orbital history (marked as red stars in the top left panel). Only particles initially associated with the LMC are plotted. The location of the SMC is denoted by a blue star. The initial state of the LMC, as a symmetric disk with flocculant spiral structure is illustrated in the panel marked $T = 0.7$ Gyr. As the SMC orbits about the LMC, asymmetric spiral structure is induced. After 4.6, 5.7, and 6.3 Gyr of evolution the SMC is roughly 25 kpc from the LMC, which is the approximate separation of the Clouds today. The last panel illustrates the final state of the system, after the SMC has been completely consumed by the LMC.

As seen in Figure 5, a dominant one-armed spiral is induced after each pericentric approach of the SMC and sometimes the structures appear more symmetric. However, the asymmetry and strength of the spiral arm is strongest after the SMC passes through the disk itself, particularly at pericenter approaches <10 kpc (e.g., $T = 6.3$). The structure in the panel marked $T = 6.3$ Gyr is most reminiscent to the observed structure in the LMC. Multiple spiral arms are formed in the region marked B and a sub-dominant arm is seen in the south, analogous to that observed (see Figure 3). The northern-most structures reach as far as 15 kpc from the LMC center (Region A), like the arc seen by Mackey et al. (2015). The mass resolution of the simulation is $2500 M_{\odot}$/particle. This is insufficient to create detailed star count maps to compare against the Mackey et al. (2015) observations, but the stellar density in the outskirts drops sharply by roughly an order of magnitude from 10 to 20 kpc, also as observed (Region B). This simulation illustrates that Milky Way tides are not necessary to form low density stellar arcs in the outskirts of the LMC that are similar to those observed.

During each off-center impact, the SMC passes through the LMC disk with a different orientation and impact location. Regardless, asymmetric spiral structures occur each time with a negligible dependence on impact time or dynamical phase of the LMC disk, as seen in more generic simulations of non-coplanar low-mass impactors (Berentzen et al. 2003). In this simulation we adopted a total mass ratio of $M_{\rm SMC}/M_{\rm LMC} = 0.1$, which provided the best match to both dynamical mass constraints of the Clouds and the global properties of the Magellanic System (Besla et al. 2010). In addition, Berentzen et al. (2003) have shown that similar asymmetric spiral structures can form from encounters between galaxies with mass ratios as high as 0.2. The existence of these spiral structures is thus a general prediction of eccentric encounters with low mass companions and is not strongly dependent on the exact orbital solution depicted here.

However, the exact orientation, strength and number of resulting spiral structures in the LMC do change depending on the impact parameter and number of encounters with the SMC, meaning the existence of these structures may be a way of constraining the LMC–SMC interaction history. From this study, a direct collision ($b < 10$ kpc) appears necessary to reproduce the observed asymmetry of the outer spiral morphology of the LMC. The structure induced from a wide separation passage ($T = 4.6$ Gyr) are more symmetric, reminiscent of the simulations presented in Mackey et al. (2015) of the impact of global Milky Way tides.

3.2. The LMC and SMC About the Milky Way

In the previous section we illustrated that close interactions between the LMC and SMC ($b < 10$ kpc) are sufficient to create asymmetric spiral arms and arcs in the outskirts of the LMC disk that are similar to those observed. Here we include the Milky Way to assess the degree to which the tidal field of the Galaxy is affecting this picture.

We turn to simulations of the Clouds and Milky Way that reproduce both the internal structure of the LMC and the major components of the extended Magellanic System (i.e., Bridge and Stream): Model 2 of B12. In this model the Clouds have just passed their first pericentric approach to a $1.5 \times 10^{12}\ M_{\odot}$ Milky Way (a distance of ~49 kpc Besla et al. 2007) and the SMC has recently collided with the LMC ~0.1 Gyr ago to form the Magellanic Bridge (impact parameter $b < 5$ kpc). As illustrated in Figures 5 and 6 of Besla et al. (2013), there is stellar debris from the SMC surrounding the LMC disk (see also Olsen et al. 2011) and also strong perturbations to both the outskirts and inner regions of the LMC disk in this model.

In the left hand panel of Figure 6 we plot the stellar density of particles originally associated with the LMC at the present time in Galactic coordinates (1 Gyr after the LMC crosses R200 of the Milky Way, i.e., the distance where the dark matter density of the Milky Way's halo is 200 times the critical density. Debris from the SMC is predicted to be more diffusely distributed behind and about the LMC disk (Besla et al. 2013) and does not contribute to the prominent stellar arcs seen in the outskirts of the simulated LMC disk. White contours highlight structures in the inner disk, including a one-armed spiral and geometrically off-center bar—these structures do not form without a low impact parameter collision between the Clouds (Berentzen et al. 2003, B12). The green region (5°–8° north of the center of the bar, marked C) is analogous to the northern structures visible in our imaging campaign (Figures 3 and 1). The density of the disk drops sharply outside a radius of 10° (Region B). The northern-most arc structure (marked A, located ~15° from the bar) is an order of magnitude less dense than region B and may be similar to the structure observed by Mackey et al. (2015). In particular, it appears to protrude from a different direction than the inner arms, which may be caused by the combined effect of warping by the global tidal field of the MW and viewing geometry. Notably, there is no southern counterpart to this structure. These structures are analogous to those described in Figure 5, where the Clouds interact in isolation (no Milky Way).

Here, tidal forces from both the SMC and Milky Way are acting on the LMC disk at this point in the simulation. Milky Way tides must play a role in shaping the stellar debris at the largest radii, however that does not imply that tides from the Galaxy originally formed the structures. To determine the origin of the northern-most stellar arc (A) in the left-hand panel of Figure 6, we tag particles associated with this structure at the present time and trace them back to an earlier point in time.

In the right hand panel of Figure 6 we plot the stellar density of the LMC disk ~0.7 Gyr ago (~0.3 Gyr after the LMC

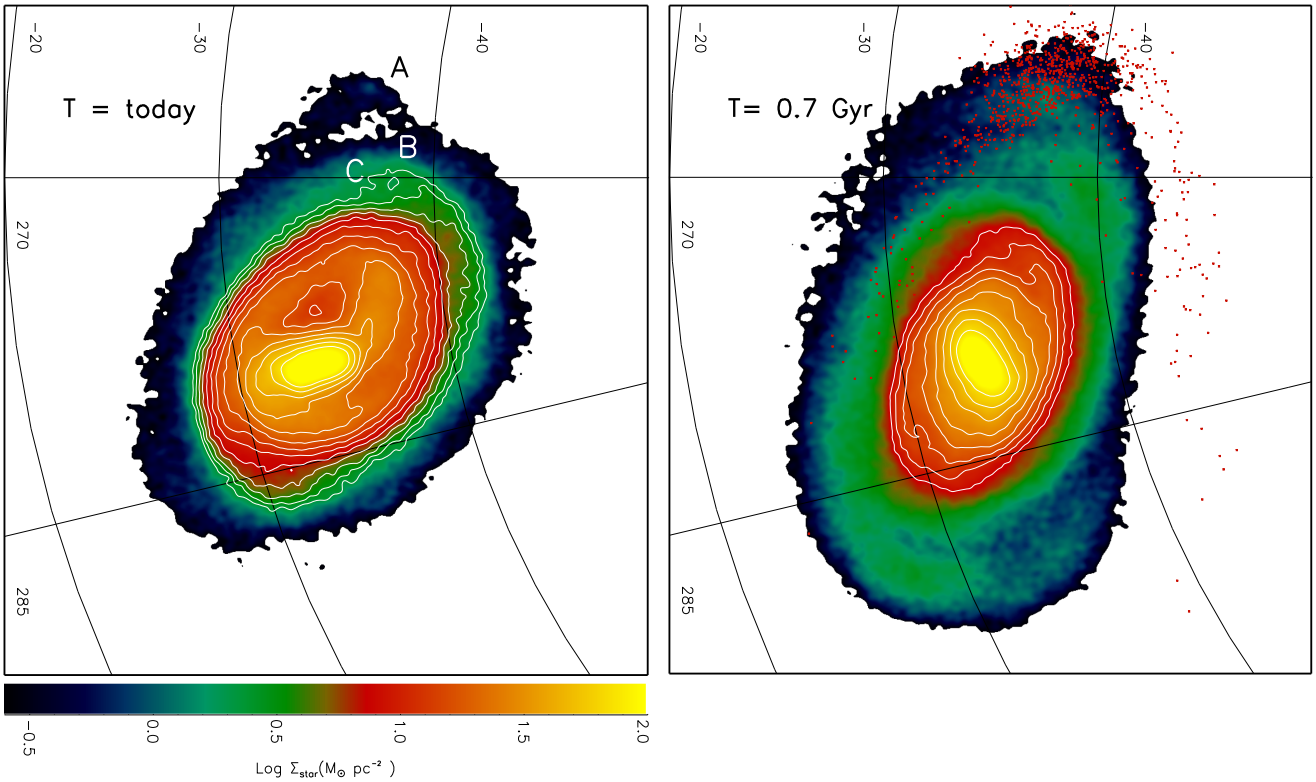

Figure 6. Left: stellar density of the simulated LMC disk from B12 in Galactic coordinates at the present time (1 Gyr after the LMC crossed R200 of the Milky Way). White contours highlight the inner disk structure, which consists of a one-armed spiral and off-center stellar bar in the higher density regions (red) and arcs in the lower density region C, analogous to those revealed by our deep imaging campaign (Figure 3). The northern-most stellar arc (Region A) is similar to the low-density structure identified by Mackey et al. (2015) and is located ∼15° from the LMC center. The stellar density drops sharply in Region B. Right: the simulated LMC disk 0.7 Gyr ago, well before the pericentric approach of the LMC to the Milky Way, which occurred <50 Myr ago. The disk has been placed at the current location of the LMC to facilitate a line of sight comparison with the present day disk. As such, lines of Galactic latitude are only drawn for reference. Red dots illustrate the location of stellar particles that ultimately end up in arc A. These red particles are located in arms of the outer disk that were perturbed by the SMC at distances where Milky Way tides are negligible.

crossed R200 of the Milky Way). At this point Milky Way tides are minimal as the LMC is located ∼170 kpc from the Galactic center. For the sake of comparison, the figure illustrates how the LMC disk would look like from the same distance and viewing perspective as the LMC today (left panel). Red dots mark the location of stellar particles associated with arc A from the left panel. The outskirts of the LMC disk are highly disturbed by SMC tides (recall, Milky Way tides are negligible). Indeed the simulated disk asymmetries are similar to those in Figure 5.

Given the much smaller mass of the SMC, it is tidal field is a localized effect, versus the global perturbations induced by the Milky Way, thus giving rise to the pronounced asymmetry in the resulting tidal structures. While the final shape of the structure may be influenced by Milky Way tides after the recent pericentric approach of the LMC, the stellar arc originates from LMC stars in the outskirts of the disk that are initially tidally disturbed by the SMC during previous passages, implying the existence of a long-lived LMC–SMC binary system.

While writing this paper it became clear that the LMC disk model in the B12 was not inclined correctly with regards to our line of sight. The inclination has been corrected for the line of sight images shown in Figure 6; however it should be noted that as a result the SMC is not in the correct location on the plane of sky. As such, the exact orientation of the stellar arcs in the northern regions should not be interpreted as precise predictions. Also, our understanding of the 3D velocities of the LMC have changed since the B12 simulations were created (Kallivayalil et al. 2013). But a first infall scenario remains the most plausible scenario for Milky Way mass models with virial masses $<1.5 \times 10^{12}\ M_{\odot}$ and total LMC masses in excess of $10^{11} M_{\odot}$, as explored in this study (Kallivayalil et al. 2013).As such, the change in velocity does not affect the general conclusions drawn in this section.

4. DISCUSSION: CONNECTION TO MAGELLANIC IRREGULAR GALAXIES

Many Magellanic Irregular dwarf galaxies, i.e., analogs of the LMC, are known to have low mass companions (Odewahn 1994; Wilcots & Prescott 2004; Pearson et al. 2016). Classic examples include NGC 4490/85, UGC 9562/60, NGC 3448/UGC 6016. Each of these dwarf pairs also possess connecting HI bridges, analogous to the Magellanic Bridge (Noreau & Kronberg 1986; Clemens et al. 1998; Cox et al. 2001) and extended HI envelopes that are unlikely to arise owing to ram pressure or perturbations from a massive companion as these systems are relatively isolated (Pearson et al. 2016). It is thus postulated that the off-center stellar bar and highly asymmetric spiral structure that characterize the Magellanic Irregular galaxy class (de Vaucouleurs & Freeman 1972) may result from interactions with a companion dwarf galaxy (Berentzen et al. 2003; Besla et al. 2012; Yozin & Bekki 2014). Indeed many Magellanic Irregular galaxies are not in proximity to a massive host galaxy (e.g., Arp22).

The results shown in Figures 5 and 6 are consistent with previous theoretical studies of minor mergers and we expect them to be generically applicable to LMC analogs in the field. For example, Berentzen et al. (2003) modeled the stellar structure of barred Milky Way like galaxies during collisions with smaller galaxies. They similarly conclude that off-center impacts can induce one-armed spiral structure (see also similar studies by: Lynds & Toomre 1972; Weil & Hernquist 1993; Athanassoula et al. 1997; Struck 1997).

Figure 5 further illustrates that extreme impact parameters (<5 kpc) are not a necessary condition to reproduce the broad morphology of the outer stellar disks of Magellanic Irregulars. In the specific case of the LMC, at least one close impact is likely required to reproduce the LMC's inner disk morphology in detail, particularly that of the stellar bar. B12 showed that an off-center SMC impact ($b \sim 2$–5 kpc) can warp the bar out of the LMC disk plane, consistent with observations (Haschke et al. 2012). A 10 kpc impact, as illustrated by the panel marked $T = 6.3$ Gyr, is able to reproduce the outer spiral morphology, but the bar is still coplanar with the disk.

A major argument against the B12 picture that interactions between dwarfs are responsible for the disturbed nature of Magellanic Irregulars is that many do not have obvious companions (Wilcots & Prescott 2004). But, perhaps surprisingly, Figure 5 illustrates that, while many of the outer stellar structures are transient, the dominant one-armed spiral persists even after the SMC is completely cannibalized at $T = 8.0$ Gyr! A 1:10 mass ratio merger[9] is insufficient to destroy the disk of the LMC. This result is consistent with results from studies of minor mergers on disk stability for more massive, gas rich systems (e.g., Bournaud et al. 2005; Hopkins et al. 2008; Moster et al. 2012). As such, the final merged system, when signs of a companion are minimal, maintains the appearance of a Magellanic Irregular galaxy.

The LMC–SMC merger simulation was run until 9.2 Gyr, revealing that the one-armed spiral structure dissipates within 1–2 Gyr of coalescence. Please see the accompanying movie of the simulation for reference. These structures are thus hallmarks of a very recent or ongoing minor merger. Indeed, the Magellanic Irregular galaxy NGC 4449 was thought to be isolated until a low surface brightness companion was found in its periphery (Martínez-Delgado et al. 2012). We expect that similar deep imaging campaigns about other Magellanic Irregulars are likely to reveal stellar signatures of tidal disturbances.

The *TiNy Titans Survey*, a multi-wavelength survey of the gas and star formation properties of pairs of dwarf galaxies (Stierwalt et al. 2015), demonstrated that star formation is enhanced in paired dwarfs over isolated counterparts. Our study further develops this picture, highlighting the role that dwarf–dwarf interactions can play in the morphological evolution of these low mass systems. The expected frequency of such interactions can be estimated from cosmological simulations, and is the subject of ongoing work (G. Besla et al. 2016, in preparation).

5. CONCLUSIONS

Recent deep observations of the stellar periphery of the LMC have been published using data from the Dark Energy Survey identifying a stellar arc or stream in the very outskirts of the LMC (∼15° from the center of the LMC) (Mackey et al. 2015). These authors suggest that Milky Way tides may be responsible for the origin of this structure. However, the DES footprint does not cover the southern regions of the LMC outer disk, where the (Mackey et al. 2015) models predict that complementary structures should exist. Furthermore, these data do not examine the structure of the LMC disk from radii of 5–10 kpc which could influence the origin of structure in the very outskirts.

In this study we present deep, high-resolution, optical images of the Magellanic System using low cost robotic telescopes with wide fields of view to explore stellar substructure in the outskirts of the stellar disk of the LMC (5°−10° from the center). These high resolution data build upon the seminal work of deVF72, which were the first team to identify that substantial structure exists in the outskirts of the LMC. Our data has confirmed the existence of stellar arcs and multiple spiral arms in the northern periphery, with no comparable counterparts in the south. The asymmetry of these structures disfavors a formation scenario driven by global Milky Way tides. Galactic cirrus is minimal in the north and unlikely to affect interpretation of these observations.

We have compared these data to detailed simulations of the LMC disk resulting from interactions with its low mass companion, the SMC, in isolation and with the inclusion of the Milky Way tidal field in order to assess the origin of these northern structures, including the Mackey et al. (2015) stellar arc at ∼15°.

We conclude that repeated close interactions with the SMC are primarily responsible for the asymmetric stellar structures induced in the periphery of the LMC, particularly the dominant one-armed spiral and multiple spiral arms or arcs in the northern disk. This is clearly illustrated in the panel marked $T = 6.3$ Gyr in Figure 5, where the LMC is seen to be highly distorted owing to the tidal field of the SMC alone. A movie of this simulation is available with the online version of this paper.

While Milky Way tides likely influence the final distribution of structures in the outskirts, the origin of structures such as the distant arc identified by Mackey et al. (2015) is likely a relic of the past LMC–SMC interaction history. Testing this model would require similarly deep observations of the southern outskirts of LMC disk; comparable structures should exist if the origin of this structure is Milky Way tides. The upcoming DECam Magellanic Satellites Survey (PI: Bechtol) will extend the DES footprint to the south and should shed more light on this scenario.

These new data, particularly the properties of the arcs in the north, thus provide powerful new constraints that will allow us to narrow down the orbital parameter space and understand in detail the recent interaction history of the Magellanic Clouds. In particular, these data can help constrain the longevity of the LMC/SMC binary state. Such comparisons of high resolution, deep optical data and simulated stellar structure of a generic 1:10 mass ratio dwarf galaxy encounter provides a strong illustration of how dwarf–dwarf interactions can fundamentally modify the stellar structure of dwarf galaxies like the LMC.

Outer spiral arms and arcs are found to be transient, but the dominant one-armed spiral induced by a collision between dwarfs would persist for 1–2 Gyr even after the secondary merges entirely with the primary. As such, the lack of a

[9] Note that the mass ratio is larger at the final stages of coalescence as much of the dark matter mass of the SMC was placed in an extended halo, which is easily truncated by LMC tides.

companion around a Magellanic Irregular does not disprove the hypothesis that the structures defining this class of galaxy (one-armed spiral and geometrically off-center bar) are driven by interactions with low mass companions. Instead, such stellar structures are hallmarks of ongoing interactions or a recent merger event. Deep, wide-field observations of the outer peripheries of Magellanic Irregulars may thus harbor clues to test this theoretical picture.

We thank Dougal Mackey and David Schminovich for useful conversation that have improved this manuscript. GB acknowledges support through HST AR grant #12632. Support for program #12632 was provided by NASA through a grant from the Space Telescope Science Institute, which is operated by the Association of Universities for Research in Astronomy, Inc., under NASA contract NAS 5-26555. DMD and EKG acknowledge support by Sonderforschungsbereich (SFB) 881 "The Milky Way System" of the German Research Foundation (DFG), particularly through subproject A2. ES acknowledges support for this work provided by NASA through Hubble Fellowship grant HST-HF2-51367.001-A awarded by the Space Telescope Science Institute, which is operated by the Association of Universities for Research in Astronomy, Inc., for NASA, under contract NAS 5-26555. This paper is based on observations made at the La Silla Paranal Observatory. The simulations in this paper were produced on the Odyssey cluster supported by the FAS Science Division Research Computing Group at Harvard University. Analysis was undertaken on the El Gato cluster at the University of Arizona, which is supported by the National Science Foundation under Grant No. 1228509.

REFERENCES

Abraham, R. G., & van Dokkum, P. G. 2014, PASP, 126, 55
Amorisco, N. C., Martínez-Delgado, D., & Schedler, J. 2015, arXiv:1504.03697
Athanassoula, E., Puerari, I., & Bosma, A. 1997, MNRAS, 286, 284
Balbinot, E., Santiago, B. X., Girardi, L., et al. 2015, MNRAS, 449, 1129
Bechtol, K., Drlica-Wagner, A., Balbinot, E., et al. 2015, ApJ, 807, 50
Belokurov, V., & Koposov, S. 2016, MNRAS, 456, 602
Berentzen, I., Athanassoula, E., Heller, C. H., & Fricke, K. J. 2003, MNRAS, 342, 343
Besla, G. 2015, arXiv:1511.03346
Besla, G., Hernquist, L., & Loeb, A. 2013, MNRAS, 428, 2342
Besla, G., Kallivayalil, N., Hernquist, L., et al. 2007, ApJ, 668, 949
Besla, G., Kallivayalil, N., Hernquist, L., et al. 2010, ApJ, 721, 97
Besla, G., Kallivayalil, N., Hernquist, L., et al. 2012, MNRAS, 421, 2109
Bica, E., Bonatto, C., Dutra, C. M., & Santos, J. F. C. 2008, MNRAS, 389, 678
Bournaud, F., Jog, C. J., & Combes, F. 2005, A&A, 437, 69
Boylan-Kolchn, M., Besla, G., & Hernquist, L. 2011, MNRAS, 414, 1560
Casetti-Dinescu, D. I., Vieira, K., Girard, T. M., & van Altena, W. F. 2012, ApJ, 753, 123
Clemens, M. S., Alexander, P., & Green, D. A. 1998, MNRAS, 297, 1015
Cox, A. L., Sparke, L. S., Watson, A. M., & van Moorsel, G. 2001, AJ, 121, 692
de Vaucouleurs, G., & Freeman, K. C. 1972, VA, 14, 163
Diaz, J., & Bekki, K. 2011, MNRAS, 413, 2015
Drlica-Wagner, A., Bechtol, K., Rykoff, E., et al. 2015, ApJ, 813, 109
Duc, P.-A., Cuillandre, J.-C., Karabal, E., et al. 2015, MNRAS, 446, 120
Gómez, F., Besla, G., Carpintero, D. D., et al. 2015, ApJ, 802, 128
Graff, D. S., Gould, A. P., Suntzeff, N. B., Schommer, R. A., & Hardy, E. 2000, ApJ, 540, 211
Harris, J. 2007, ApJ, 658, 345
Haschke, R., Grebel, E. K., & Duffau, S. 2012, AJ, 144, 106
Hindman, J. V., Kerr, F. J., & McGee, R. X. 1963, AuJPh, 16, 570
Hopkins, P. F., Hernquist, L., Cox, T. J., Younger, J. D., & Besla, G. 2008, ApJ, 688, 757
Kallivayalil, N., van der Marel, R. P., Besla, G., Anderson, J., & Alcock, C. 2013, ApJ, 764, 161
Kerr, F. J. 1957, AJ, 62, 93
Koerwer, J. F. 2009, AJ, 138, 1
Kontizas, M., Morgan, D. H., Hatzidimitriou, D., & Kontizas, E. 1990, A&AS, 84, 527
Koposov, S. E., Belokurov, V., Torrealba, G., & Evans, N. W. 2015, ApJ, 805, 130
Kunkel, W. E., Demers, S., Irwin, M. J., & Albert, L. 1997, ApJL, 488, L129
Lah, P., Kiss, L. L., & Bedding, T. R. 2005, MNRAS, 359, L42
Lynds, R., & Toomre, A. 1972, ApJ, 209, 382
Mackey, D., Koposove, S. E., Erkal, D., et al. 2015, arXiv:15508.1356
Martin, N. F., Nidever, D. L., Besla, G., et al. 2015, ApJL, 804, L5
Martínez-Delgado, D., Gabany, R. J., Crawford, K., et al. 2010, AJ, 140, 962
Martínez-Delgado, D., Peñarrubia, J., Gabany, R. J., et al. 2008, ApJ, 689, 184
Martínez-Delgado, D., Romanowsky, A. J., Gabany, R. J., et al. 2012, ApJL, 748, L24
Mathewson, D. S., Cleary, M. N., & Murray, J. D. 1974, ApJ, 190, 291
McMonigal, B., Bate, N. F., Lewise, G. F., et al. 2014, MNRAS, 444, 3139
Meschin, I., Gallart, C., Aparicio, A., et al. 2014, MNRAS, 438, 1067
Mihos, C. J., Harding, P., Feldmeier, J., & Morrison, H. 2005, ApJ, 631, 41
Moretti, M. I., Clementini, G., Muraveva, T., et al. 2014, MNRAS, 437, 2702
Moster, B. P., Maccó, A. V., Somerville, R. S., Naab, T., & Cox, T. J. 2012, MNRAS, 423, 2045
Moster, B. P., Naab, T., & White, D. M. 2013, MNRAS, 428, 3121
Muñoz, R. R., Majewski, S. R., Zaggia, S., et al. 2006, ApJ, 649, 201
Nidever, D. L., Majewski, S. R., Muñoz, R. R., et al. 2011, ApJ, 733L, 10
Nidever, D. L., Majewsky, S. R., Burton, W. B., & Nigra, L. 2010, ApJ, 723, 1618
Nikolaev, S., Drake, A. J., Keller, S. C., et al. 2004, ApJ, 601, 260
Noreau, L., & Kronberg, P. P. 1986, AJ, 92, 1048
Odewahn, S. C. 1994, AJ, 107, 1320
Olsen, K. A. G., & Salyk, C. 2002, ApJL, 656, L61
Olsen, K. A. G., Zaritsky, D., Blum, R. D., Boyer, M. L., & Gordon, K. D. 2011, ApJ, 737, 29
Pearson, S., Besla, G., Putman, M. E., et al. 2016, arXiv:1603.09342
Peñarrubia, J., Gómez, F., Besla, G., Erkal, D., & Ma, Y.-Z. 2016, MNRAS, 456, 54
Putman, M. E., Staveley-Smith, L., Freeman, K. C., Gibson, B. K., & Barnes, D. G. 2003, ApJ, 586, 170
Rubele, S., Girardi, L., Kerber, L., et al. 2015, MNRAS, 449, 639
Růžička, A., Theis, C., & Palouš, J. 2010, ApJ, 725, 369
Saha, A., Olszewski, E. W., Brondel, B., et al. 2010, AJ, 140, 1719
Salem, M., Besla, G., Bryan, G., et al. 2015, ApJ, 815, 77
Schlegel, D. J., Finkbeiner, D. P., & Davis, M. 1998, ApJ, 500, 525
Springel, V. 2005, MNRAS, 364, 1105
Stierwalt, S., Besla, G., Patton, D., et al. 2015, ApJ, 805, 2
Struck, C. 1997, ApJS, 113, 269
Subramaniam, A. 2003, ApJL, 598, L19
Udalski, A., Szymański, M. K., & Szymański, G. 2015, AcA, 65, 1
van der Marel, R. P. 2001, AJ, 122, 1827
van der Marel, R. P., & Cioni, M.-R. L. 2001, AJ, 122, 1807
van Dokkum, P. G., Abraham, R., & Merritt, A. 2014, ApJ, 782, 24
van Dokkum, P. G., Abraham, R., Merritt, A., et al. 2015, ApJ, 798, 45
Weil, M. L., & Hernquist, L. 1993, ApJ, 405, 142
Wilcots, E. M., & Prescott, M. K. M. 2004, AJ, 127, 1900
Yozin, C., & Bekki, K. 2014, MNRAS, 439, 1948